Plant Molecular Biology (2020) 103:173–184
https://doi.org/10.1007/s11103-020-00982-4

MEDEA-interacting protein LONG-CHAIN BASE KINASE 1 promotes pattern-triggered immunity in *Arabidopsis thaliana*

Priya Gupta[1] · Shweta Roy[1] · Ashis Kumar Nandi[1]

Received: 29 August 2019 / Accepted: 20 February 2020 / Published online: 25 February 2020

Key message **Arabidopsis LONG-CHAIN BASE KINASE 1 (LCBK1) interacts with MEDEA, acomponent of PCR2 complex that negatively regulates immunity. LCBK1 phosphorylatesphytosphingosine and thereby promotes stomatal immunity against bacterial pathogens.**

Abstract Arabidopsis polycomb-group repressor complex2 (PRC2) protein MEDEA (MEA) suppresses both pattern-triggered immunity (PTI) and effector-triggered immunity (ETI). MEA represses the expression of *RPS2* and thereby attenuates *AvrRpt2* effector-mediated ETI. However, the mechanism of MEA-mediated PTI diminution was not known. By screening the Arabidopsis cDNA library using yeast-2-hybrid interaction, we identified LONG-CHAIN BASE KINASE1 (LCBK1) as an MEA-interacting protein. We found that *lcbk1* mutants are susceptible to virulent bacterial pathogens, such as *Pseudomonas syringae* pv *maculicola* (*Psm*) and *P. syringae* pv *tomato* (*Pst*) but not the avirulent strain of *Pst* that carries *AvrRpt2* effector. Pathogen inoculation induces *LCBK1* expression, especially in guard cells. We found that LCBK1 has a positive regulatory role in stomatal closure after pathogen inoculation. WT plants close stomata within an hour of *Pst* inoculation or flg22 (a 22 amino acid peptide from bacterial flagellin protein that activates PTI) treatment, but not *lcbk1* mutants. LCBK1 phosphorylates phytosphingosine (PHS). Exogenous application of phosphorylated PHS (PHS-P) induces stomatal closure and rescues loss-of-PTI phenotype of *lcbk1* mutant plants. MEA overexpressing (MEA-Oex) plants are defective, whereas loss-of-function *mea-6* mutants are hyperactive in PTI-induced stomatal closure. Exogenous application of PHS-P rescues loss-of-PTI in MEA-Oex plants. Results altogether demonstrate that LCBK1 is an interactor of MEA that positively regulates PTI-induced stomatal closure in Arabidopsis.

Keywords ETI · Phytosphingosine · PTI · Stomatal immunity

Introduction

Plants are capable of activating immunity against invading pathogens. They recognize molecular patterns present in the microbes through pattern-recognition receptors (PRRs) to activate the immune response. Structural components of microbial pathogens, such as bacterial flagellin protein, lipopolysaccharides, fungal cell wall chitin, and oomycete glycoproteins, are examples of patterns that activate PTI in plants (Zhang and Zhou 2010). Successful pathogens release effector molecules to suppress pattern-triggered immunity (PTI). Plants also evolved recognition system against specific effectors for activating a stronger immunity, known as effector-triggered immunity (ETI). Activation of the immune response in plants involves a large number of receptors, transactivators, transcription factors, chromatin-modelers, biosynthetic enzymes, kinases, phytohormones, antibiotic peptides, and other phytochemicals. Plants recruit both positive and negative regulator defense for fine-tuning the output of defense response. Activation of immunity takes place at the cost of metabolic energy. Negative regulators help to keep the immunity expression at an optimal level (Huot et al. 2014).

Arabidopsis polycomb-group repressor complex2 (PRC2) component MEDEA (MEA) functions as a negative regulator of defense against bacterial and fungal pathogens (Roy et al. 2018). MEA primarily regulates female gametophyte

Electronic supplementary material The online version of this article (https://doi.org/10.1007/s11103-020-00982-4) contains supplementary material, which is available to authorized users.

✉ Ashis Kumar Nandi
ashis_nandi@yahoo.com

[1] School of Life Sciences, Jawaharlal Nehru University, 415, New Delhi 110067, India

and endosperm development (Grossniklaus et al. 1998). MEA is genetically imprinted for which, only maternal copy of the gene expresses in female gametophyte and endosperm (Kinoshita et al. 1999). However, pathogen inoculation results in ectopic expression of MEA in vegetative tissues, which is required for controlling defense response activation (Roy et al. 2018). MEA over-expression plants show reduced PTI against virulent pathogens and ETI induced by the avirulent *Pst* strain that carries bacterial effector protein AvrRpt2 (*Pst-AvrRpt2*). Experiments suggested that Di19 protein recruits MEA at *RPS2* locus for epigenetic suppression, and the reduced *RPS2* expression results attenuated ETI against *Pst-AvrRpt2* (Roy et al. 2018). However, the mechanism of MEA-mediated suppression of PTI was not known. Our work identified the possible involvement of MEA in PTI-induced stomatal opening.

The entry of a pathogen into the host system is a crucial step for successful colonization. In plants, bacterial pathogens use the stomatal route for gaining entry into the host leaves. Plants are capable of closing stomata upon recognition of pathogens, whereas bacteria reinforce stomatal opening with the help of effector molecules (Melotto et al. 2006). A conserved 22 aminoacid fragment of flagellin protein (flg22) is perceived by the FLS2 receptor for activating PTI in Arabidopsis (Gomez-Gomez and Boller 2000; Chinchilla et al. 2006). Exogenous application of flg22 induces stomatal closure in WT but not in *fls2* mutant (Melotto et al. 2006), suggesting the association of stomatal closure with PTI activation. Like other PTI responses, stomatal closure is also suppressed by effectors. Bacterial pathogen *Pseudomonas syringae* pv *tomato* DC3000 (*Pst*) can reopen stomata after 3 h of inoculation (Melotto et al. 2006). *Pst* secretes coronatine toxin inside the host cell. Experiments suggest that the reopening of stomata by *Pst* is a coronatine-dependent response (Melotto et al. 2006). Abscisic acid (ABA) is the most critical plant hormone for regulating stomatal aperture during biotic and abiotic stress. In addition to ABA, other components like NO, H_2O_2, lipopolysaccharides (LPS), and phytosphingosine regulate stomatal closure during abiotic stress (Sah et al. 2016). In contrast to ABA-mediated stomatal closure, the mechanism of stomatal aperture control during plant-pathogen interaction is less known. Here, we report that LONG-CHAIN BASE KINASE 1 (LCBK1), which was identified as an interacting factor of MEA, positively regulates stomatal immunity in Arabidopsis.

Materials and methods

Plant materials and growth condition

MEA over-expression and mutant lines are described earlier (Roy et al. 2018). The T-DNA insertion mutants *lcbk1-2* (Salk_152371C) and *lcbk1-3* (SAIL_529_H04) were obtained from Arabidopsis Biological Resource Centre, Ohio State University, USA. Plants were grown in a growth room at 22 °C and 65% relative humidity with an alternate light /dark period of 12 h each as described previously (Roy et al. 2018).

Generation of *lcbk1*-complemented lines

LCBK1 gene, along with introns, was amplified from Arabidopsis Col-0 genomic DNA and cloned under cauliflower mosaic virus 35S promoter in pCXSN vector (Chen et al. 2009) and mobilized into *Agrobacterium tumefaciens* C58 strain. The *lcbk1-2* mutant plants were transformed by the floral dip method, and transgenic plants were selected on hygromycin (25 ppm) plate. Primers used are mentioned as Supplementary Table S1.

Pathogen inoculation, phytosphingosine (PHS), phytosphingosine-1-phosphate (PHS-P), and flg22 treatment

Pathogen inoculation and method of determination of bacterial load were described previously (Singh et al. 2014). In brief, over-night grown bacterial cultures were resuspended in 10 mM $MgCl_2$ at the required concentration (described under each experiment). Leaves of 5-week-old Arabidopsis plants were inoculated either by pressure infiltration with a needle-less syringe or by spraying on both abaxial and adaxial surfaces. Typically, we inoculated 12 to 15 plants per line and 2 to 3 leaves per plant. For PHS (Avanti Polar Lipid Cat# 860499) and PHS-P (Avanti polar lipids Cat# 860491) treatment, plants were sprayed with PHS or PHS-P solution made in ethanol: DMSO (2:1), with or without pathogen (control). For flg22 treatment, flg22 peptide (Gen script Cat No RP19986) was dissolved in water and pressure infiltrated into the abaxial side of leaves.

DAB staining

Leaves along with petiole were detached at 15 h-post-inoculation and floated on distilled water for 2 h. Further, distilled water was replaced by DAB staining solution (1 mg/ml in 10 mM Na_2HPO_4) and vacuum (5 mm Hg pressure) infiltrated for 5 min. Leaves dipped in DAB solution was kept for 4 to 5 h for staining at room temperature. Destaining was done in 95% ethanol and photographs were taken (Roy and Nandi 2017).

RNA isolation, cDNA synthesis, and expression analysis

Total RNA extraction, cDNA preparation, and quantitative real-time PCR (qPCR) were carried out as described

earlier (Giri et al. 2017; Roy et al. 2018). Typically, 1.0 µg of DNAse-treated total RNA was used for cDNA preparation using a cDNA synthesis kit (Bio-Rad; catalog # 170-8891). qPCR was carried out by BioRad (CFX connect) system with gene-specific primers (Supplementary Table S1) and 2 × SYBR Green master mix (Bio-Rad; catalog no. #172-5124). Each experiment contained three biological samples at each time point with two technical replicates. The average of the two technical replicates was taken for the calculation. Relative expression levels were determined after normalization with *TUBULIN2* (*At5g62690*) and *ACTIN2* (*At3g18780*). The melting curve generated by the software was used to ensure the presence of a single PCR product in each sample.

Bimolecular fluorescence complementation (BiFC)

BiFC constructs were generated by cloning coding sequences in pSPYNE(R)173 or pSPYCE(M) vector (Waadt et al. 2008) and were transformed in *Agrobacterium tumefaciens* C58 strain. Fresh onion pieces with epidermal peel were fully immersed in *A. tumefaciens* suspension (0.8 OD) and kept at 28 °C for 6–8 h. Onion pieces were then transferred on half-strength Murashige and Skoog medium (Sigma-Aldrich, India, Cat# M5519) and incubated for 2–3 days. Cocultivated scales were thoroughly washed with sterile water. The epidermal layer was peeled off, stained with appropriate dye and mounted on a slide using 20% glycerol for observation. Samples were observed under a confocal microscope and analyzed with the Olympus FV1000 viewer software.

Yeast two-hybrid library screening

The *MEDEA* CDS was cloned into the pBGKT7 vector between *Eco*RI and *Bam*HI restriction sites to fuse with the *GAL4* transcription factor DNA-binding domain. Screening of the Y2H Arabidopsis cDNA library (Clontech, USA, Cat # 630489) was done as described earlier (Banday and Nandi 2018; Roy et al. 2018).

Stomatal aperture measurement

Leaf peels from the abaxial side of Arabidopsis young leaves were floated in the stomatal buffer (MES-KOH-10 mM, KCl-30 mM; pH 6.15) for 2.5 h under the light. Treatments for testing stomatal aperture included *Pst* at 10^8 CFU/ml, flg22 5 µM, ABA 10 µM, PHS 10 µM, or PHS-P 10 µM. PHS and PHS-P stock solutions were made as 1 mM in ethanol:DMSO (2:1), ABA stock solution was prepared as 10 mM in methanol, and others were made in water and diluted in the stomatal buffer. After treatment, epidermal peels were further incubated under light from 30 min to 3 h, as mentioned under the respective figure legends and observed under a light microscope. Stomatal apertures of 80 to 100 stomata, randomly taken from microscopic views, were measured using ImageJ software (Arnaud et al. 2017).

LCBK1:GUS expression study

About 1.8 kb upstream region from the translational start site of *LCBK1* was cloned into the pCAMBIA1303 vector between *Bam*HI and *Spe*I restriction sites. pCAMBIA 1303 and *LCBK1*:*GUS* construct was transformed in *Agrobacterium tumefaciens* C58 strains. Transient GUS activity in Arabidopsis leaves was done as described earlier (Lee and Yang 2006). In brief, 4-week-old Arabidopsis leaves were first infiltrated with *Agrobacterium tumefaciens* containing either *35S:GUS* or *LCBK1:GUS* (0.4 OD) construct. After 48 h, the same leaves were infiltrated with *Pst* (10^5 CFU/ml suspended in 10 mM $MgCl_2$) or only 10 mM $MgCl_2$ as the mock. After 12 h of the second infiltration, GUS staining was carried out as described previously (Roy et al. 2018). Whole leaf and epidermal peels were put in the GUS staining solution separately. The microscopic view of epidermal peels was observed after overnight GUS staining.

Callose deposition

Arabidopsis leaves were infiltrated with either *Pst* (5×10^8 CFU/ml) or flg22 (1 µM), and samples were collected at 10 hpi and incubated overnight in 95% ethanol solution. Leaves were stained with 0.01% aniline blue solution (in 1.5 mM Na_2HPO_4 pH 9) for 10 h, photos were taken in the light microscope, and callose spots were counted using ImageJ software (Singh et al. 2018).

Results

LCBK1 physically interacts with MEA

To gain insight into the mechanism of MEA-mediated suppression of PTI (Roy et al. 2018), we screened MEA-interacting proteins from the Arabidopsis cDNA library by yeast-2-hybrid assay and selected three interactors having putative roles in controlling PTI. These interactors were VOLTAGE DEPENDENT ANION CHANNEL-2 (VDAC2), NDR1/HIN1-LIKE 3 (NHL3), and LONG-CHAIN BASE KINASE 1 (LCBK1 Fig. 1a). Arabidopsis VDAC2 and NHL3 promote basal defense against virulent bacterial pathogens (Varet et al. 2003; Singh et al. 2018). The role of LCBK1 in plant immune response was not known. LCBK1 codes for a sphingosine kinase (Imai and Nishiura 2005). Phosphorylation of phytosphingosine (PHS) is associated with stomatal closure after ABA treatment (Coursol et al. 2005), which

is also a component of plant immune response (Su et al. 2017). To study the role of LCBK1 in immune response, we first confirmed the interaction between MEA and LCBK1 *in planta* by bimolecular fluorescence complementation assay (BiFC) in onion (*Allium cepa*) epidermal cells. LCBK1 and MEA coding sequences were transcriptionally fused with N- and C- terminal of fragments of yellow fluorescent protein (YFP) present in pSPYNE and pSPYCE vector respectively (Waadt et al. 2008). These fusion constructs were transiently expressed in onion epidermal layer and fluorescence was observed under a confocal microscope. pSPYNE-CBL1 and pGMAS-CIPK24 were used as a positive control which was known to interact on the plasma membrane (Waadt et al. 2008). Results suggested that MEDEA interacts with LCBK1 on the plasma membrane (Fig. 1b). Only vectors, along with MEA were used as the negative control (Supplementary Fig. S1).

LCBK1 expression is pathogen inducible

To investigate the association of *LCBK1* expression with the activation of the immune response, we monitored LCBK1 mRNA accumulation after *Pseudomonas syringae* pv *tomato* DC3000 (*Pst*; suspended in 10 mM $MgCl_2$) inoculation or only 10 mM $MgCl_2$ (mock) in WT Arabidopsis plants. We observed significantly enhanced expression of *LCBK1* in *Pst* inoculated leaves compared to mock-treated samples (Fig. 2a, b), which suggests that *LCBK1* expression is induced upon pathogen inoculation. To further validate, we monitored *LCBK1* promoter-driven GUS reporter (*LCBK1:GUS*) expression. We cloned GUS reporter under 1.8 kb upstream sequences of *LCBK1* and transiently expressed in Arabidopsis leaves. As a control, we used cauliflower mosaic virus *35S:GUS*. We observed high-level expression of *LCBK1:GUS* after pathogen treatment, which was negligible without pathogen (Fig. 2c).

Sphingosine kinase, for example, SPHK1 is involved in ABA-induced stomatal closure via phosphorylation of PHS (Coursol et al. 2005). PHS can also be phosphorylated by LCBK1 (Imai and Nishiura 2005). Thus, we hypothesize that LCBK1 might be induced in the guard cells and also be involved in stomatal movements after pathogen attack. To check the inducibility of *LCBK1* in guard cells, we infiltrated the *LCBK1:GUS* construct in Arabidopsis leaves with

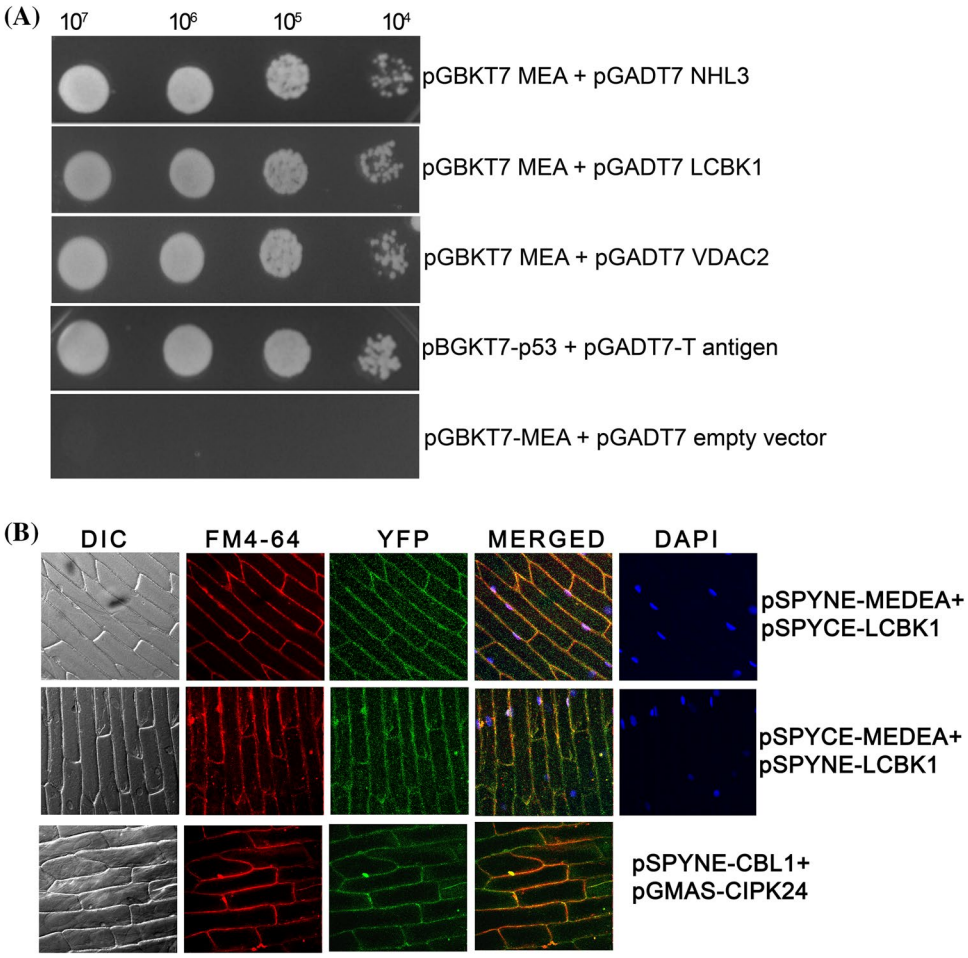

Fig. 1 Physical interaction between MEA and LCBK1. **a** Yeast two-hybrid interaction. Transformed yeast cells were grown on Leu−, Trp−, His−, , and Ade− (−LTHA) medium, which allows only interacting clones to grow. pGBKT7- p53 and pGADT7 -T antigen were used as positive controls; pGBKT7-MEA and pGADT7 empty vector was used as negative controls. Overnight-grown yeast cells were suspended at 10^7 yeast/ml and serially diluted before spotting on the selection medium. Photographs were taken after 3 days of growth at 28 °C. **b** Bimolecular fluorescence complementation (BiFC) assay in transiently expressed onion epidermal cells. pSPYNE-CBL1 and pGMAS-CIPK24 were used as a positive control

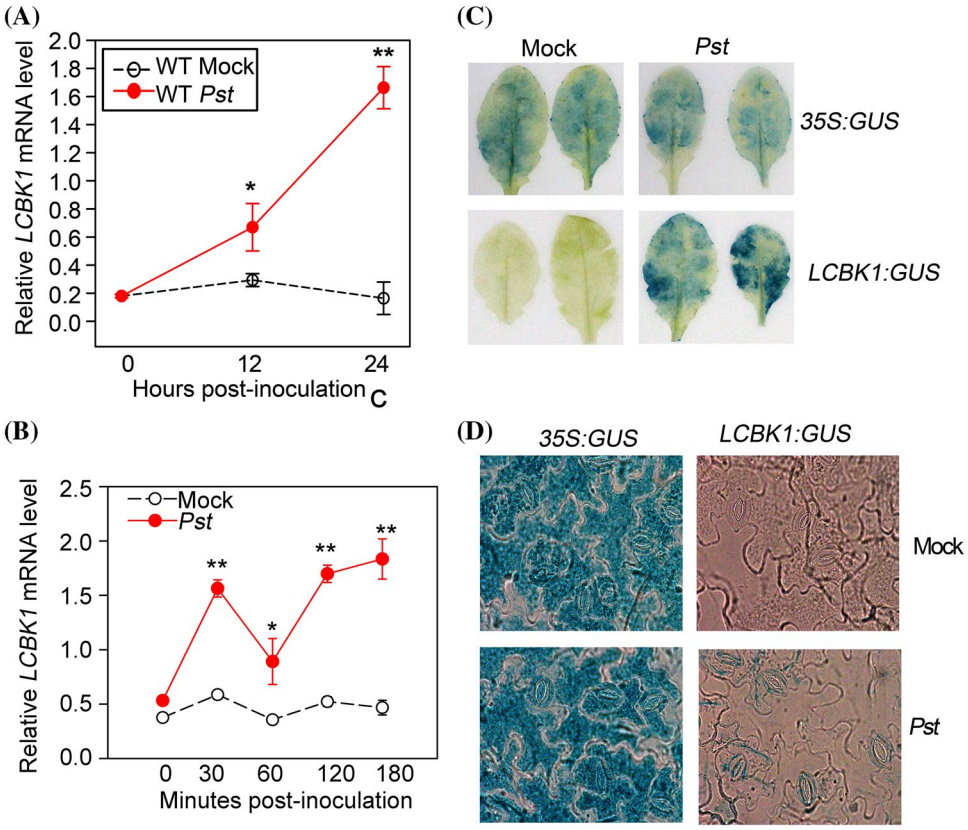

Fig. 2 *LCBK1* expression. **a**, **b** qRT-PCR to show *LCBK1* transcript accumulation after mock or *Pst* inoculation. Each point in the line plot represents ± S.D. of three biological replicates having two technical replicates. *($P < 0.05$) and **($P < 0.001$) indicate the mean values of *LCBK1* transcripts after pathogen inoculation are significantly different from mock-treated samples as determined by student's *t*-test. **c** *35S:GUS* or *LCBK1:GUS* activity in Arabidopsis leaves after *Pst* or mock inoculation. **d** GUS staining in the WT epidermal peel of Arabidopsis transiently expressing *35S:GUS* or *LCBK1:GUS*. In each experiment, *Pst* was suspended in 10 mM $MgCl_2$ at 10^6 CFU/mL and only 10 mM $MgCl_2$ was used as mock

or without *Pst* inoculation. Epidermal layers were excised and stained for GUS expression. We found a significantly high level of GUS expression in guard cells than other epidermal cells after pathogen treatment (Fig. 2d). However, *LCBK1:GUS* expression is not restricted to guard cells, as evident from the Fig. 2c and d.

LCBK1 promotes PTI

We studied the role of LCBK1 in disease defense in two T-DNA insertion lines SALK_152371 (referred to as *lcbk1-2*) (Huang et al. 2017), and SAIL_529_H04 (referred to as *lcbk1-3*) obtained from Arabidopsis Biological Resource Centre (ABRC). In *lcbk1-2* and in *lcbk1-3* the T-DNA insertions are in 7th exon and 4th intron respectively (Supplementary Fig. S2A). The presence of the T-DNA was confirmed by standard PCR techniques (Supplementary Fig. S2B, C). T-DNA insertion lines do not accumulate *LCBK1* transcript as determined by reverse-transcription PCR (RT-PCR) (Supplementary Fig. S2D). *TUB2* expression was used as a control for the RT-PCR experiment. We did not observe any morphological defect in these mutants (Supplementary Fig. S2E). We studied apoplastic immunity by infiltrating and stomatal immunity by spraying pathogens on leaves of WT and *lcbk1* mutant plants. The *npr1-1* mutant was used as a control. We observed that *lcbk1-2* and *lcbk1-3* mutant supported more bacterial growth and developed a higher level of disease symptoms than WT plants after the infiltration of the virulent bacterial pathogen *Pseudomonas syringae* pv *maculicola* ES4326 (*Psm*) (Fig. 3a). A similar loss-of-resistance phenotype in *lcbk1* mutants was observed after spraying *Psm* into the leaves (Fig. 3b). To further confirm, we tested immunity against another virulent pathogen, *P. syringae* pv *tomato* DC3000 (*Pst*). We found that both the allelic *lcbk1* mutant lines supported more bacterial growth and showed more severe symptoms than WT plants after *Pst* infiltration (Fig. 3c) or spraying (Fig. 3d). Results suggested that LCBK1 is a positive regulator of both stomatal and apoplastic immunity in Arabidopsis. To further ascertain, we generated transgenic plants expressing LCBK1 in the *lcbk1-2* mutant background (Supplementary Fig. S3). The expression of LCBK1 rescued the loss-of-resistance phenotype in *lcbk1-2* plants (Fig. 3e). Activation of PTI results enhanced callose deposition. In agreement with the reduced defense against virulent pathogens, we observed reduced callose deposition in *lcbk1* after *Pst* inoculation or treatment with flg22 (Fig. 3f, Supplementary Fig. S4), a part of bacterial flagellin protein that activates PTI in Arabidopsis (Gomez-Gomez and Boller 2000). Reduced immunity in *lcbk1* is also associated with the reduced expression of *PR1* gene (Fig. 3g), and apoplastic ROS production (Fig. 3h). We also studied the role of LCBK1 in ETI by challenging

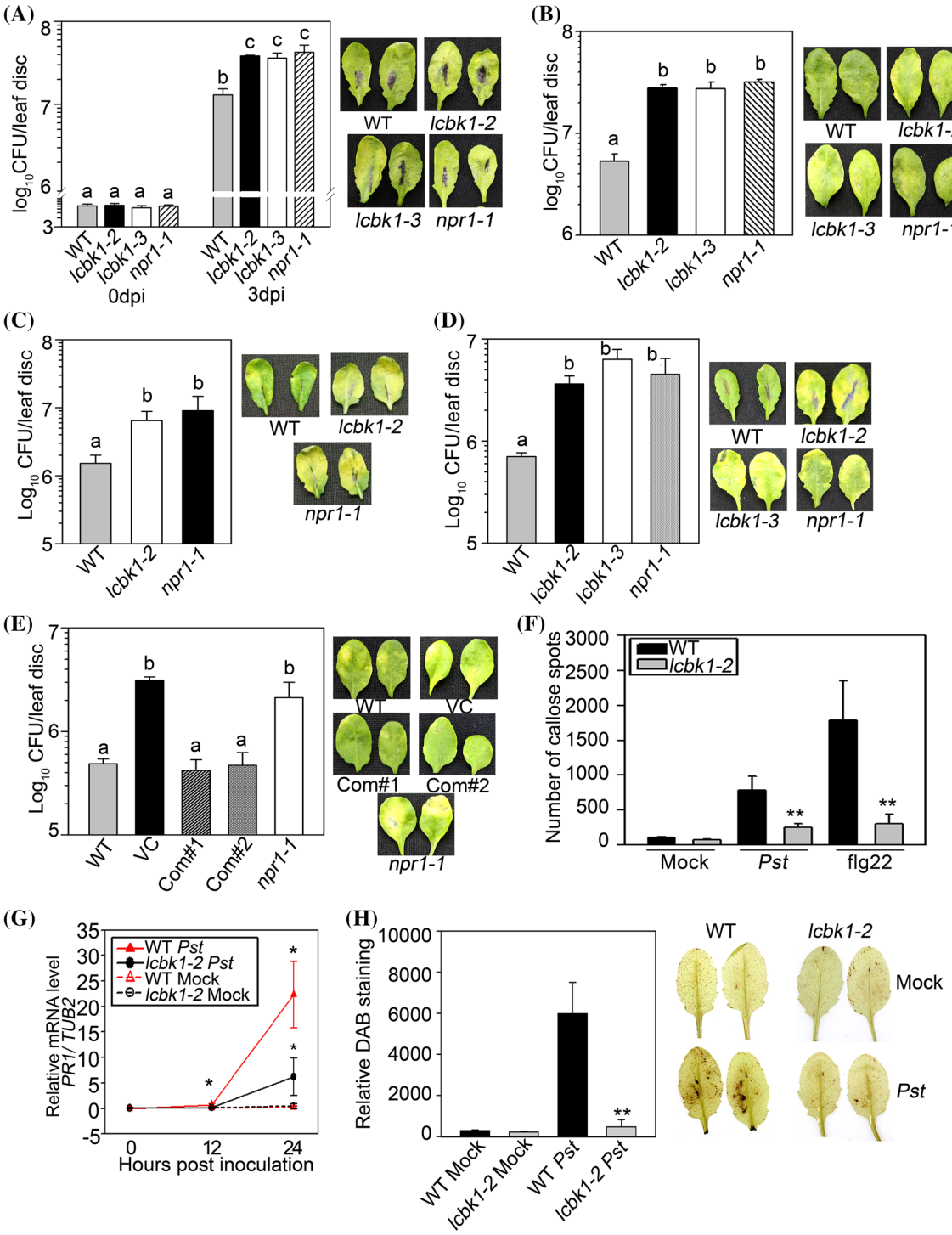

Fig. 3 PTI in WT and *lcbk1* mutant. **a** *Psm* counts and disease symptoms in the indicated genotypic plants. *Psm* was pressure infiltrated at 5×10^5 CFU/ml. **b** *Psm* counts and disease symptoms after 4 days of spray inoculation at 5×10^8 CFU/ml. **c** *Pst* counts, and disease symptoms after 3 days of pressure infiltration at 5×10^5 CFU/ml. **d** *Pst* counts, and disease symptoms after 4 days of spray inoculation at 5×10^8 CFU/ml. **e** *Pst* count, and disease symptoms after 4 days of spray inoculation at 5×10^8 in. WT, empty vector transformed control (VC), LCBK1 complemented (Com), and *npr1-1* plants. In A to E, each bar represents mean ± S.D. (n = 4). Different letters above the bars indicated a statistically significant difference ($P<0.001$) as obtained by one-way ANOVA (Holm-Sidak method). **f** Callose deposition after *Pst* and flg22 treatment after 10 h post-inoculation (hpi). Each bar represents the mean ± SD (n = 10). **g** Relative *PR1* transcript level after *Pst* inoculation (at 5×10^5 CFU/ml) in *lcbk1-2* and WT, as determined by qPCR. Each point in the line plot represents mean ± S.D. (n = 3). **h** ROS production in WT and *lcbk1-2* mutant at 12 h-post *Pst* inoculation (5×10^5 CFU/ml). Each bar represents the mean ± SD (n = 5). *($P<0.05$) and **($P<0.001$) indicate the mean values that are significantly different from WT samples as determined by student's *t*-test

with the avirulent pathogen *Pst* carrying *AvrRpt2* effector (*Pst*-AvrRpt2). Contrary to the enhanced growth of the virulent pathogen in *lcbk1-2*, no difference was observed in the bacterial count between WT and *lcbk1-2* after *Pst-AvrRpt2* spray or infiltration inoculation (Supplementary Fig. S5). The above results suggested that LCBK1 promotes resistance against virulent pathogens and promote PTI.

LCBK1 is required for pathogen-induced stomatal closure

To investigate the role of LCBK1 in stomatal defense, we monitored pathogen-induced stomatal aperture in *lcbk1-2* mutant and WT plants. Activation of PTI leads to rapid closure of stomata. (Melotto et al. 2006, 2017). Coronatine secreted by *Pseudomonas syringae* leads to the reopening of stomata after initial closure (Melotto et al. 2006). We also observed stomatal closure in *Pst*-treated WT leaves in 1 h, which reopens at three hours post-inoculation (Fig. 4a). In contrast to WT, the *lcbk1-2* leaves were not able to close stomata after pathogen inoculation. Additionally, no difference was found in stomatal aperture size after mock and *Pst* treatment in *lcbk1-2* at both the time points. In contrast to pathogen inoculation, activation of PTI by flg22 allows retaining of stomata in a closed state for a more extended period of time (Fig. 4b; Melotto et al. 2006, 2017). However, we observed no significant difference in stomatal aperture between flg22 or mock-treated *lcbk1-2* samples, suggesting the involvement of LCBK1 in stomatal immunity. We also applied ABA on epidermal peels of WT and *lcbk1-2* to study ABA-induced stomatal closure. As expected, exogenous application of ABA resulted in a reduction in the stomatal aperture in WT plants (Supplementary Fig. S6). The *lcbk1* mutant also responded to the ABA application, but the stomatal opening was bigger than WT, suggesting that ABA-mediated stomatal closure is partially dependent on LCBK1.

Phytosphingosine-phosphate (PHS-P) but not phytosphingosine (PHS) induce stomatal closure in WT and *lcbk1* mutants

LCBK1 encodes a sphingosine kinase that specifically phosphorylates D-erythro-dihydrosphingosine (DHS), but not N-acetyl-DHS or D-threo-DHS. It also phosphorylates D-erythro-sphingosine, trans-4, trans-8-sphingadienine (found exclusively in plants) and phytosphingosine (PHS) (Imai and Nishiura 2005). PHS level increases in Arabidopsis leaves within one hour after *Pst* inoculation (Peer et al. 2010). Results described in the previous section (Fig. 4a and b) showed that *lcbk1-2* is defective in stomatal immunity. To gain an insight into the mechanism of stomatal defense pathway, we checked the effect of phytosphingosine (PHS) and phosphorylated-phytosphingosine (PHS-P) on the

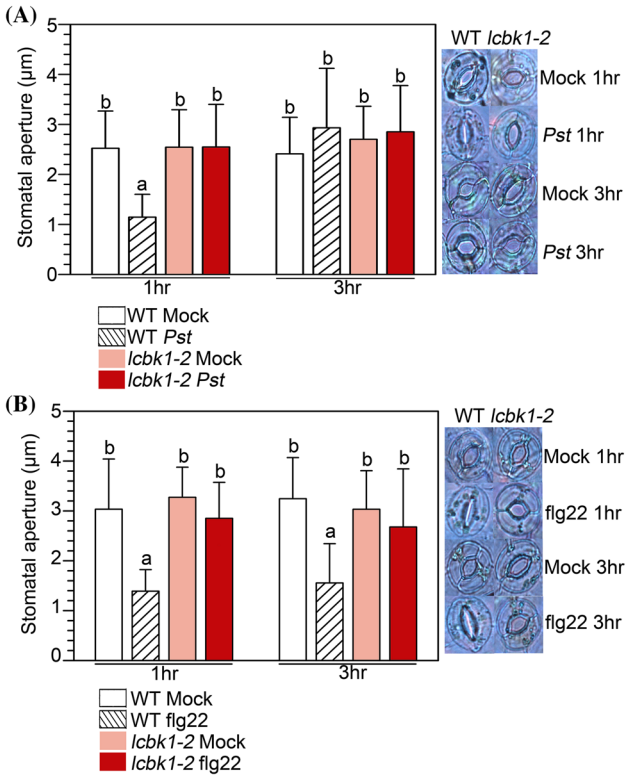

Fig. 4 Pathogen-induced stomatal closure in WT and *lcbk1* plants. Stomatal aperture sizes were observed through microscopy at 1 h and 3 h post-inoculation in WT and *lcbk1-2* with *Pst* (**a**) flg22 (**b**). Each bar represents the mean ± SD (n = ~80). Different letters above the bars indicated a statistically significant difference ($P < 0.001$) as obtained by one-way ANOVA (Holm-Sidak method)

flg22-mediated stomatal aperture of *lcbk1-2*. We observed that PHS application does not affect stomatal opening in WT or *lcbk1* mutant plants when applied alone (Fig. 5a) or in combination with flg22 (Fig. 5b). However, the application of PHS-P alone was sufficient for closing stomata both in WT and *lcbk1-2* mutant (Fig. 5c), and flg22 application does not alter PHS-P-mediated stomata closure (Fig. 5d). Thus, phosphorylation of PHS is a downstream event of flg22-mediated stomatal closure. Results demonstrated that phosphorylation of PHS mediated by LCBK1 is essential for closing the stomata during pathogen attack.

Exogenous application of PHS-P rescues pathogen-susceptibility of *lcbk1-2*

The results described above suggest that PHS-P is able to close the stomata in *lcbk1-2*. So we wanted to check whether PHS-P is able to rescue the susceptible phenotype of *lcbk1-2*. To examine this hypothesis, we sprayed the WT and *lcbk1-2* with different combinations like Mock+*Pst*, PHS+*Pst,* and PHS-P+*Pst*. We observed that bacterial load is high in *lcbk1-2* after mock and PHS-treated plants

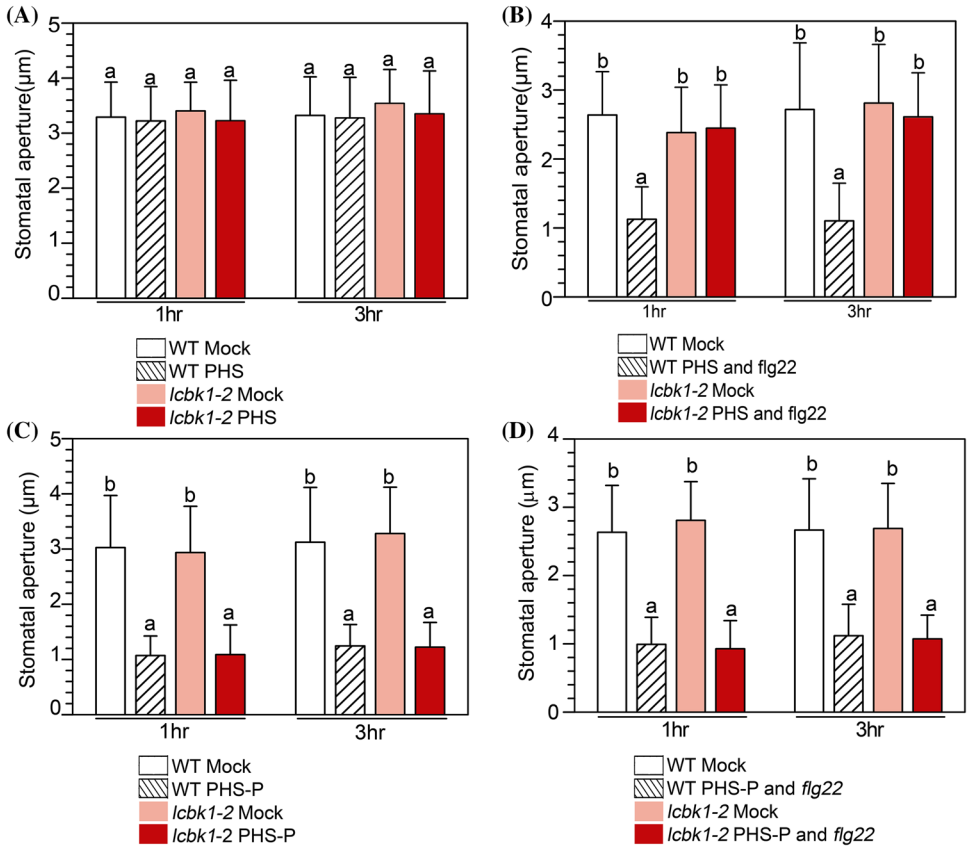

Fig. 5 Effect of phytosphingosine (PHS) and phytosphingosine -1-phosphate (PHS-P) on the stomatal aperture of WT and *lcbk1*. **a** Mock and PHS treatment; **b** Mock and flg22+PHS treatment; **c** Mock and PHS-P treatment; **d** Mock and PHS-P+flg22 treatment. Each bar represents the mean ± SD (n = ~80). Different letters above the bars indicated a statistically significant difference ($P < 0.001$) as obtained by one-way ANOVA (Holm-Sidak method)

as compared to WT while bacterial load in PHS-P treated *lcbk1-2* plant is almost similar to WT treated with mock (Fig. 6a). The *lcbk1* mutant plants are also defective in PTI-induced callose deposition (Fig. 3f). To examine whether PHS-P can rescue the callose deposition defect of *lcbk1-2* plants, we infiltrated PHS-P along with Pst or flg22 and monitored callose deposition. PHS-P application alone induced callose deposition only to a modest level in WT or *lcbk1-2* plants (Fig. 6b). However, when applied along with *Pst* or flg22, PHS-P completely rescued callose deposition defect of *lcbk1-2* plants (Fig. 6b). The results demonstrated that PHS-P is able to rescue the susceptible phenotype of *lcbk1-2* and is required for closing the stomata as a defense response during pathogen attack.

MEA negatively regulates stomatal immunity

The previous report suggested that the *mea-6* mutant plants were resistant, and MEA-Oex lines were susceptible to *Pst* (Roy et al. 2018). Here, we already discussed that LCBK1 has a positive role in stomatal defense and it interacts with MEA at the plasma membrane. Thus, we checked the role of MEA in stomatal defense. We treated *mea-6* and C24 (WT) epidermal peels with flg22 (Fig. 7a) and *Pst* (Fig. 7b). We found that both *mea-6* and WT were able to close the stomata after flg22 treatment, but there was a significant difference in the stomatal aperture size between them. WT has a wider stomatal aperture than *mea-6* after both 1 h and 3 h post-inoculation. Additionally, we also observed a similar pattern in both WT and *mea-6* after *Pst* treatment. We observed stomata reopens during late hours of *Pst* inoculation in WT plants due to coronatine toxin released by the pathogen, but it remains closed in *mea-6* at 3 h-post-inoculation. Hence, we observed an increased difference in the stomatal aperture size in WT and *mea-6* at 3 h post-inoculation of *Pst*. Further, we treated the epidermal peels of WT and MEA-Oex lines (Line no #1,#3 and #6) with flg22 (Fig. 7c) and checked the stomatal aperture size. Similar to *lcbk1-2* plants, flg22-treated MEA-Oex epidermal peels also showed a defect in stomatal closure. Interestingly, the application of PHS-P activates stomatal closure in MEA-Oex plants as does for WT plants (Fig. 7d). The results altogether suggest that MEA being associated with LCBK1 inactivates its function, which results in a loss of stomatal defense and PTI.

PHS-P application restores loss-of-defense against *Pst* in MEA-Oex plants

MEA-Oex plants are susceptible to *Pst* (Fig. 8; Roy et al. 2018). Exogenous application of PHS-P restores the stomatal closure defect of *lcbk1* as well as MEA-Oex plants (Figs. 5 and 7). To further confirm the role of LCBK1 in the

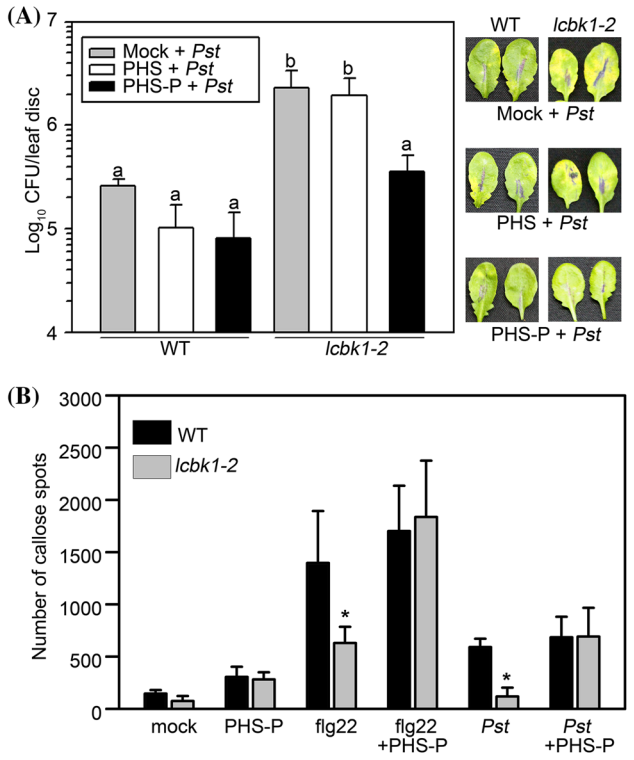

Fig. 6 PTI in WT and *lcbk1* plants after PHS or PHS-P treatment. **a** Bacterial numbers and disease symptoms in WT and *lcbk1-2* after spraying *Pst* (5×10^8 CFU/ml.) along with water (mock) or PHS or PHS-P. Bacterial colonies were counted and symptoms recorded on the fourth day after inoculation. Each bar represents the mean ± SD (n = 4). Different letters above the bars indicated a statistically significant difference ($P<0.001$) as obtained by one-way ANOVA (Holm-Sidak method). **b** Callose deposition after combinatorial treatment of *Pst* (10^6 CFU/ml), flg22 (1 µM), or PHS-P at 10 hpi. Each bar represents the mean ± SD (n = 10). *($P<0.05$) and **($P<0.001$) indicate the mean values that are significantly different from WT samples as determined by student's *t*-test

susceptibility phenotype of MEA-Oex plants, we monitored *Pst* counts after the PHS-P application. We observed that when PHS-P was sprayed along with *Pst*, *MEA*-Oex plants showed immunity similar to that of WT plants (Fig. 8). Results demonstrated the association of LCBK1 in the susceptibility phenotype of *MEA*-Oex plants.

Discussion

We identified LCBK1 as a positive regulator of basal immunity in Arabidopsis. Expression of *LCBK1* increases upon pathogen inoculation (Fig. 2). Results suggest the positive regulatory role of LCBK1 both in apoplastic and stomatal immunity. The *lcbk1* mutant plants support higher loads of virulent bacterial pathogens and are compromised for callose deposition, *PR1* gene expression, and ROS production (Fig. 3). Plant hormone ABA regulates stomatal opening, especially during abiotic stresses. However, the role of ABA in plant immunity depends on the stage of infection. At the preinvasive stage, ABA acts positively in plant resistance by enhancing stomatal immunity (Ton et al. 2009). At the post-invasive stage, ABA promotes bacterial growth by suppressing SA mediated plant defense and callose deposition. In WT plants, exogenous application of flg22 or LPS induces stomatal closure but not in ABA-deficient *aba3-1* mutant or in *open stomata 1* (*ost1*) mutant that is defective in ABA-induced stomatal closure (Melotto et al. 2006). These results indicate a connection between PTI-induced closure of stomata in the guard cell and ABA signaling pathways. However, peptide elicitor receptor1 (PEPR1) and PEPR2-mediated PTI induces stomatal closure in ABA- and OST1-independent manner (Zheng et al. 2018). In addition to ABA, SA also influences stomatal closure. SA biosynthesis mutant *eds16-2/sid2-2* and SA-deficient NahG transgenic plants were defective in PTI-induced stomatal closure (Melotto et al. 2006). Arabidopsis RIN4 protein is a negative regulator of basal immunity and a component of several R-Avr interactions. RIN4 functions along with plasma membrane H^+-ATPases to control stomatal aperture during pathogen invasion (Liu et al. 2009; Lee et al. 2015). Stomata not only regulate the entry of pathogens but also influence post-invasive immunity (Zhang et al. 2019). Thus, stomatal immunity plays a critical role in the overall basal defense of plants. The identification of LCBK1 provided a new mechanism of stomatal immunity. Exogenous application of PHS-P but not PHS induced stomatal closure in *lcbk1* plants. Though WT plants contain a functional *LCBK1* gene, its expression remains low without pathogen inoculation (Fig. 2a, b). Low basal level expression of LCBK1 in WT plants is the probable reason for not getting stomatal closure after PHS application. Nevertheless, the results demonstrated that phosphorylation of phytosphingosine is a possible mechanism for LCBK1-mediated stomatal immunity.

Our results also established the possible role of MEA in pathogen-induced stomatal closure. We found that MEA-Oex lines were defective in stomatal closure after flg22 treatment (Fig. 7). Also, *mea-6* plants were able to close the stomata for a longer period of time than WT plants after *Pst* inoculation (Fig. 7). These observations are in agreement with loss- and gain-of-PTI in MEA-Oex and mutant plants, respectively (Roy et al. 2018). However, the mechanism by which the MEA-LCBK1 complex influences stomatal aperture is not known. One probable hypothesis could be related to the orientation of cytoskeleton elements, which is critical for the closing and opening of stomata. Actin filaments become radially oriented to open the stomata (Eun and Lee 1997). In plants, ABA-mediated stomatal closure also induces rapid depolymerization and random orientation of actin filaments to close the stomata (Eun and Lee 1997). Additionally, lipid-based secondary messengers like

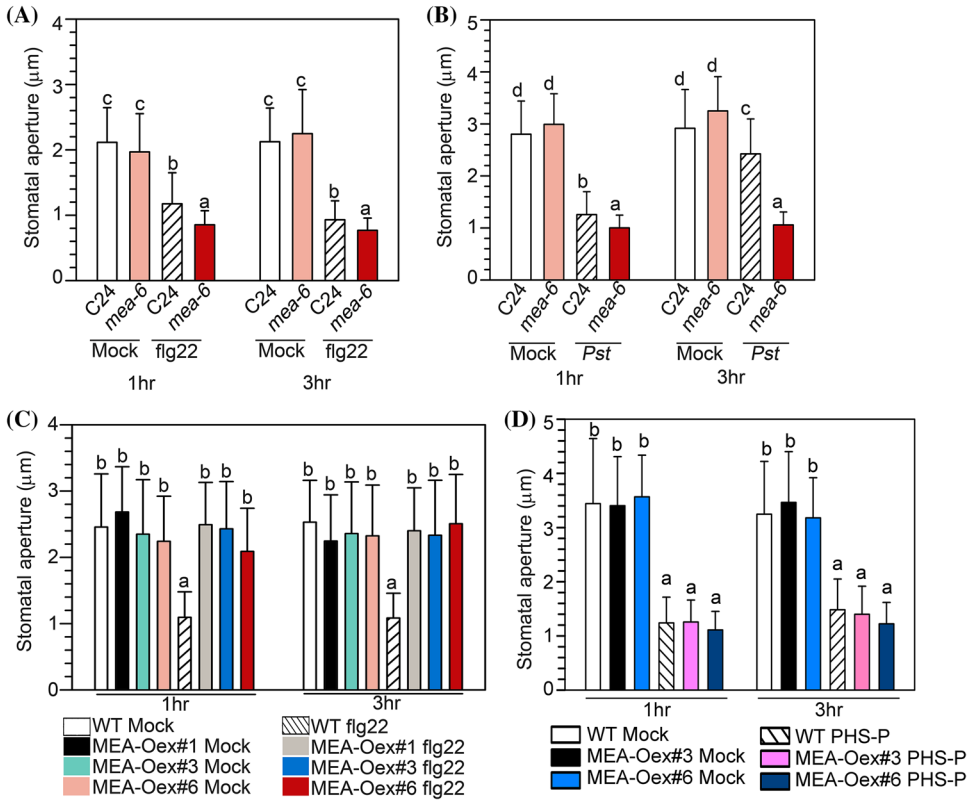

Fig. 7 Stomatal aperture in WT, MEA-Oex and *mea-6* mutant plants after *Pst,* flg22, and PHS-P treatment. **a** WT and *mea-6* after mock or flg22 treatment; **b** after mock or *Pst* inoculation; **c** WT and MEA-Oex lines after mock or flg22 treatment; **d** WT, and MEA-Oex plants after mock or PHS-P treatment. Each bar represents the mean ± SD (n = ~80). Different letters above the bars indicated a statistically significant difference ($P < 0.001$) as obtained by one-way ANOVA (Holm-Sidak method)

phosphatidylinositol 3-phosphate and phosphatidylinositol 4-phosphate are required for rearrangement of actin in guard cells and the stomatal closure triggered by ABA (Choi et al. 2008). Also, in yeast and mammals sphingolipids play an important role in actin dynamics during endocytosis (Lamaze et al. 1997; Friant et al. 2000; Zanolari et al. 2000; Dickson 2010). Moreover, in mammals, most of the interactors of cytosolic PRC2 take part in regulating actin organization. For example, Enhancer of zeste homolog-2 (EZH2), a PRC component functions as a transcriptional repressor through chromatin remodeling in Drosophila (Kuzmichev et al. 2002; Ringrose and Paro 2004). EZH2 also has been shown to interact with cytosolic proteins in megakaryocytes and T cells for regulating actin dynamics (Su et al. 2005; Roy et al. 2012). Interestingly, MEA is a structural homolog of the Enhancer of Zeste of Arabidopsis (Grossniklaus et al. 1998; Luo et al. 1999). Thus, the involvement of phytosphingosine and MEA in actin dynamics for stomatal closure is not very unlikely. MEA having a non-PRC2-like function is not surprising as well. Indeed, MEA forms a complex with FIE both in the nucleus and the cytoplasm (Oliva et al. 2016). Though the function of the cytoplasmic FIE-MEA complex is not known, a non-nuclear function beyond chromatin methylation is intuitive (Oliva et al. 2016). Our work demonstrated one non-nuclear function of MEA.

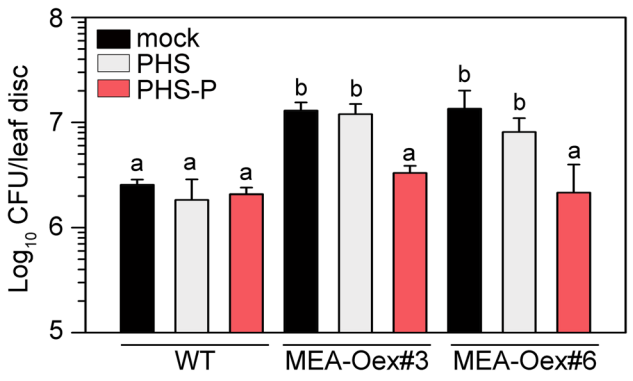

Fig. 8 *Pst* numbers in WT and MEA-Oex plants after PHS-P application. Bacterial numbers in WT and MEA-Oex plants after spraying *Pst* (5×10^8 CFU/ml) along with water (mock), or PHS, or PHS-P application. Bacterial numbers were counted on the fourth day of inoculation. Each bar represents the mean ± SD (n = 4). Different letters above the bars indicated a statistically significant difference ($P < 0.001$) as obtained by one-way ANOVA (Holm-Sidak method)

Acknowledgements We acknowledge ABRC, Ohio State University for mutant seeds. This work was supported by the Science and Engineering Research Board project (SERB/SR/SO/PS/150/2012 to AKN), and the CSIR fellowship to SR and PG.

Author contributions PG-performed most of the experiments, analyzed data, and designed some of the experiments; SR-performed some of the experiments; AN-conceptualized the designed most of the experiments.

PG and AN-wrote the manuscript, which has been further modified and approved by all authors.

References

Arnaud D, Lee S, Takebayashi Y, Choi D, Choi J, Sakakibara H, Hwang I (2017) Cytokinin-mediated regulation of reactive oxygen species homeostasis modulates stomatal immunity in arabidopsis. Plant Cell 29:543–559

Banday ZZ, Nandi AK (2018) *Arabidopsis thaliana* GLUTATHIONE-S-TRANSFERASE THETA 2 interacts with RSI1/FLD to activate systemic acquired resistance. Mol Plant Pathol 19:464–475

Chen S, Songkumarn P, Liu J, Wang GL (2009) A versatile zero background T-vector system for gene cloning and functional genomics. Plant Physiol 150:1111–1121

Chinchilla D, Bauer Z, Regenass M, Boller T, Felix G (2006) The Arabidopsis receptor kinase FLS2 binds flg22 and determines the specificity of flagellin perception. Plant Cell 18:465–476

Choi Y, Lee Y, Jeon BW, Staiger CJ, Lee Y (2008) Phosphatidylinositol 3- and 4-phosphate modulate actin filament reorganization in guard cells of day flower. Plant, Cell Environ 31:366–377

Coursol S, Le Stunff H, Lynch DV, Gilroy S, Assmann SM, Spiegel S (2005) Arabidopsis sphingosine kinase and the effects of phytosphingosine-1-phosphate on stomatal aperture. Plant Physiol 137:724–737

Dickson RC (2010) Roles for Sphingolipids in *Saccharomyces cerevisiae*. Adv Exp Med Biol 688:217–231

Eun SO, Lee Y (1997) Actin filaments of guard cells are reorganized in response to light and abscisic acid. Plant Physiol 115:1491–1498

Friant S, Zanolari B, Riezman H (2000) Increased protein kinase or decreased PP2A activity bypasses sphingoid base requirement in endocytosis. EMBO J 19:2834–2844

Giri MK, Singh N, Banday ZZ, Singh V, Ram H, Singh D, Chattopadhyay S, Nandi AK (2017) GBF1 differentially regulates CAT2 and PAD4 transcription to promote pathogen defense in *Arabidopsis thaliana*. Plant J 91:802–815

Gomez-Gomez L, Boller T (2000) FLS2: an LRR receptor-like kinase involved in the perception of the bacterial elicitor flagellin in Arabidopsis. Mol Cell 5:1003–1011

Grossniklaus U, Vielle-Calzada JP, Hoeppner MA, Gagliano WB (1998) Maternal control of embryogenesis by MEDEA, a polycomb group gene in Arabidopsis. Science 280:446–450

Huang X, Zhang Y, Zhang X, Shi Y (2017) Long-chain base kinase1 affects freezing tolerance in *Arabidopsis thaliana*. Plant Sci 259:94–103

Huot B, Yao J, Montgomery BL, He SY (2014) Growth-defense tradeoffs in plants: a balancing act to optimize fitness. Mol Plant 7:1267–1287

Imai H, Nishiura H (2005) Phosphorylation of sphingoid long-chain bases in Arabidopsis: functional characterization and expression of the first sphingoid long-chain base Kinase gene in plants. Plant Cell Physiol 46:375–380

Kinoshita T, Yadegari R, Harada JJ, Goldberg RB, Fischer RL (1999) Imprinting of the MEDEA polycomb gene in the Arabidopsis endosperm. Plant Cell 11:1945–1952

Kuzmichev A, Nishioka K, Erdjument-Bromage H, Tempst P, Reinberg D (2002) Histone methyltransferase activity associated with a human multiprotein complex containing the enhancer of Zeste protein. Genes Dev 16:2893–2905

Lamaze C, Fujimoto LM, Yin HL, Schmid SL (1997) The actin cytoskeleton is required for receptor-mediated endocytosis in mammalian cells. J Biol Chem 272:20332–20335

Lee D, Bourdais G, Yu G, Robatzek S, Coaker G (2015) Phosphorylation of the plant immune regulator RPM1-INTERACTING PROTEIN4 enhances plant plasma membrane H(+)-ATPase activity and inhibits flagellin-triggered immune responses in Arabidopsis. Plant Cell 27:2042–2056

Lee MW, Yang Y (2006) Transient expression assay by agroinfiltration of leaves. Methods Mol Biol 323:225–229

Liu J, Elmore JM, Fuglsang AT, Palmgren MG, Staskawicz BJ, Coaker G (2009) RIN4 functions with plasma membrane H+-ATPases to regulate stomatal apertures during pathogen attack. PLoS Biol 7:e1000139

Luo M, Bilodeau P, Koltunow A, Dennis ES, Peacock WJ, Chaudhury AM (1999) Genes controlling fertilization-independent seed development in *Arabidopsis thaliana*. Proc Natl Acad Sci 96:296–301

Melotto M, Underwood W, Koczan J, Nomura K, He SY (2006) Plant stomata function in innate immunity against bacterial invasion. Cell 126:969–980

Melotto M, Zhang L, Oblessuc PR, He SY (2017) Stomatal defense a decade later. Plant Physiol 174:561

Oliva M, Butenko Y, Hsieh TF, Hakim O, Katz A, Smorodinsky NI, Michaeli D, Fischer RL, Ohad N (2016) FIE, a nuclear PRC2 protein, forms cytoplasmic complexes in *Arabidopsis thaliana*. J Exp Bot 67:6111–6123

Peer M, Stegmann M, Mueller MJ, Waller F (2010) Pseudomonas syringae infection triggers de novo synthesis of phytosphingosine from sphinganine in *Arabidopsis thaliana*. FEBS Lett 584:4053–4056

Ringrose L, Paro R (2004) Epigenetic regulation of cellular memory by the Polycomb and Trithorax group proteins. Ann Rev Genet 38:413–443

Roy A, Basak NP, Banerjee S (2012) Notch1 intracellular domain increases cytoplasmic EZH2 levels during early megakaryopoiesis. Cell Death Dis 3:e380–e380

Roy S, Nandi AK (2017) *Arabidopsis thaliana* methionine sulfoxide reductase B8 influences stress-induced cell death and effector-triggered immunity. Plant Mol Biol 93:109–120

Roy S, Gupta P, Rajabhoj MP, Maruthachalam R, Nandi AK (2018) The polycomb-group repressor MEDEA attenuates pathogen defense. Plant Physiol 177:1728–1742

Sah SK, Reddy KR, Li J (2016) Abscisic acid and abiotic stress tolerance in crop plants. Front Plant Sci 7:571–571

Singh N, Swain S, Singh A, Nandi AK (2018) AtOZF1 Positively regulates defense against bacterial pathogens and NPR1-independent salicylic acid signaling. Mol Plant Microb Interact 31:323–333

Singh V, Roy S, Singh D, Nandi AK (2014) Arabidopsis flowering locus D influences systemic-acquired-resistance- induced expression and histone modifications of WRKY genes. J Biosci 39:119–126

Su IH, Dobenecker M-W, Dickinson E, Oser M, Basavaraj A, Marqueron R, Viale A, Reinberg D, Wülfing C, Tarakhovsky A (2005) Polycomb group protein Ezh2 controls actin polymerization and cell signaling. Cell 121:425–436

Su J, Zhang M, Zhang L, Sun T, Liu Y, Lukowitz W, Xu J, Zhang S (2017) Regulation of stomatal immunity by interdependent functions of a pathogen-responsive MPK3/MPK6 cascade and abscisic acid. Plant Cell 29:526–542

Ton J, Flors V, Mauch-Mani B (2009) The multifaceted role of ABA in disease resistance. Trends Plant Sci 14:310–317

Varet A, Hause B, Hause G, Scheel D, Lee J (2003) The Arabidopsis NHL3 gene encodes a plasma membrane protein and its overexpression correlates with increased resistance to *Pseudomonas syringae* pv. tomato DC3000. Plant Physiol 132:2023–2033

Waadt R, Schmidt LK, Lohse M, Hashimoto K, Bock R, Kudla J (2008) Multicolor bimolecular fluorescence complementation reveals simultaneous formation of alternative CBL/CIPK complexes in planta. Plant J 56:505–516

Zanolari B, Friant S, Funato K, Sutterlin C, Stevenson BJ, Riezman H (2000) Sphingoid base synthesis requirement for endocytosis in *Saccharomyces cerevisiae*. EMBO J 19:2824–2833

Zhang D, Tian C, Yin K, Wang W, Qiu JL (2019) Postinvasive bacterial resistance conferred by open stomata in rice. Mol Plant Microb Interact 32:255–266

Zhang J, Zhou JM (2010) Plant immunity triggered by microbial molecular signatures. Mol Plant 3:783–793

Zheng X, Kang S, Jing Y, Ren Z, Li L, Zhou JM, Berkowitz G, Shi J, Fu A, Lan W, Zhao F, Luan S (2018) Danger-associated peptides close stomata by OST1-independent activation of anion channels in guard cells. Plant Cell 30:1132–1146